Strain sensing based on radiative emission-absorption mechanism using dye-doped polymer optical fiber

doi: 10.1063/1.4998738

Applied Physics Letters

Strain sensing based on radiative emission-absorption mechanism using dye-doped polymer optical fiber

Cite as: Appl. Phys. Lett. **111**, 063301 (2017); https://doi.org/10.1063/1.4998738
Submitted: 22 May 2017 . Accepted: 02 August 2017 . Published Online: 09 August 2017

S. Kamimura, and R. Furukawa

Strain sensing based on radiative emission-absorption mechanism using dye-doped polymer optical fiber

S. Kamimura and R. Furukawa[a)]
Department of Engineering Science, Graduate School of Informatics and Engineering, The University of Electro-Communications, 1-5-1 Chofugaoka, Chofu, Tokyo 182-8585, Japan

(Received 22 May 2017; accepted 2 August 2017; published online 9 August 2017)

A stress sensor based on a dye-doped polymeric optical fiber is able to detect stress by simple comparison of two luminescence peaks from a pair of energy transfer organic dyes. Coumarin 540A (donor) and Rhodamine 6G (acceptor) were doped in the core and cladding of the fiber, respectively. For various laser wavelengths, the change in the near-field pattern and visible emission spectrum upon variation in the fiber bending diameter was evaluated. From a comparison with a low-numerical-aperture fiber, it is shown that the sensitivity of the sensor is controllable by optimization of the waveguide parameters. *Published by AIP Publishing.* [http://dx.doi.org/10.1063/1.4998738]

Because of their distributed sensor structure, fiber-optic (FO) strain sensors are widely used for structural monitoring. Compared to sensors based on mechanical and electrical transducers, FO sensors are more reliable and cost effective for monitoring building structures in challenging environments and for distributing targets.[1]

Conventional FO strain sensors based on fiber Bragg gratings and distributed Brillouin scattering provide the resolution of micro-strains.[1] Because they convert strain information into phase shifts, a spectral analyzing system, a well-tuned light source, and a system for temperature compensation are required.

Japan where earthquakes occur with high frequency because of its geographic location, buildings, and lifeline infrastructures of various types requires structural monitoring.[2,3] For example, the degree of damage in houses and infrastructures before and after an earthquake must be monitored. Infrastructures built for the 1964 Tokyo Olympic games, which do not necessarily satisfy current building standards, are now aged. Regardless of the structure, the degree of damage needs to be clarified in the order of priority and be treated efficiently given limited public funds.

Conventional FO sensors are not a satisfactory solution regarding the social demand because of their excessive installation costs and training requirements. Phase-shift sensors require electrical engineering and photonics knowledge for operation of the equipment and for signal analysis.

Here, we demonstrate strain detection using a different mechanism that could be used in a low-cost and simple FO strain-sensor. The principle is depicted in Fig. 1.[4] Donor/acceptor (D/A) dye pairs for the radiative emission-absorption mechanism are doped in the optical fiber core and cladding, respectively. The donor-exciting wavelength λ_{ex_D} is coupled to the core and propagates down the fiber. The donor dye in the core emits at the wavelength λ_{em_D}. At locations where stress is applied to the fiber, the deformation induces λ_{em_D} leaks to the cladding. Previously, it was shown that doping luminescent dye in the optical fiber core enhances light leakage from the core to cladding.[5] After absorbing this leaking light, the acceptor dye in the cladding emits λ_{em_A}, which is detected at the fiber output end and represents the extent of the stress load.

An advantage of this FO sensor is that it can display the stress information as a large peak shift. Figure 2 plots excitation and emission spectra of the Coumarin 540A (donor) and Rhodamine 6G (acceptor) pairs used here. The λ_{em_D} and λ_{em_A} peaks are about 100 nm apart. This difference can be detected with simple optical components instead of the spectral analysis required in conventional FO sensors. Therefore, because of its simple structure and mechanism, it could be easily analyzed in various types of situations at low installation and/or operational costs.

Polymer optical fibers (POFs) were used because of their low processing temperatures, which allow a wider range of heat-sensitive dye pairs to be used.[6] Most organic dyes cannot withstand the processing temperatures needed for silica fibers.[7] Another advantage of using POFs is their high elasticity, which offers a higher stress resolution than that expected from materials having low elasticity.

Here, we report on the fabrication of POFs with D/A dye pairs doped in the core and cladding, respectively, and analyze the outputs for stressed/non-stressed situations. Measurements were performed for different λ_{ex_D} and λ_{ex_A} values, or either, to demonstrate the sensor principles. Macro-bending of the fiber was used to apply stress to the POF.[8]

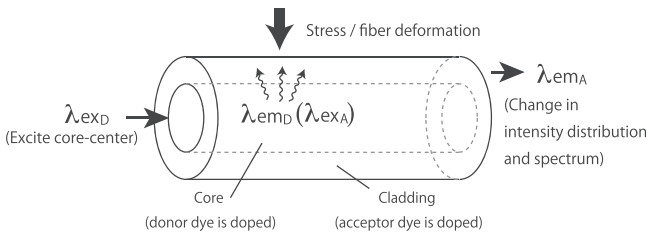

FIG. 1. Principle of the FO strain sensor using the radiative emission-absorption mechanism. λ_{ex_D}, λ_{em_D}, λ_{ex_A}, and λ_{em_A} are the emission (em) and excitation (ex) wavelengths of the donor (D) and acceptor (A) dyes. λ_{em_D} leaks to the cladding because of stress deformation and is detected by the observation of λ_{em_A} at the output.

[a)]Electronic mail: fururei@uec.ac.jp

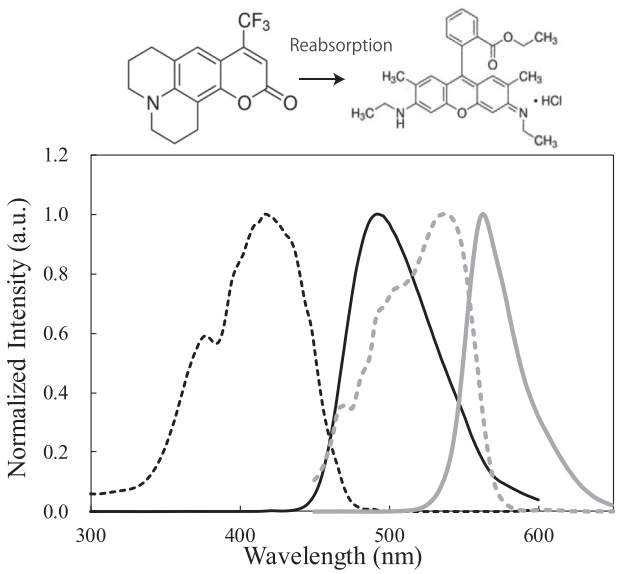

FIG. 2. Excitation (dashed curves) and emission (solid curves) spectra of Coumarin 540A (donor) and Rhodamine 6G (acceptor) in a PMMA host. Each dye was dispersed at a concentration of 0.001 wt. %.

Prior to the POF synthesis, the D/A dye concentrations to be doped in the host polymer were optimized. Coumarin 540A and Rhodamine 6G were selected as the donor and acceptor dyes, respectively, to satisfy three factors: (1) large overlap of the em_D and ex_A peaks; (2) high quantum yields; and (3) good solubility in the host monomer. Rhodamine 6G was selected as the acceptor because it is commercially available, has a high quantum yield, and was easily dispersed in methyl methacrylate (MMA) to make a POF preform.[9–11]

Coumarin 540A was selected because its emission overlaps the excitation of Rhodamine 6G and it is also soluble in MMA. Its emission peak ranges over 500–547 nm in several solvents.[12–18]

The optimum concentration of dyes doped in PMMA was determined by acquiring fluorescence spectra. Figure 2 plots the excitation and emission spectra of 0.001 wt. % Coumarin 540A and Rhodamine 6G in bulk PMMA. Major peak distortions or shifts that may suggest dye aggregation were not observed. Considering the pronounced peaks, the concentration is adequate to obtain high fluorescence intensity and was thus adopted for POF fabrication.

The POFs were fabricated from preforms according to the interfacial gel polymerization method reported by Koike *et al.*[19] As was done previously, 11 wt. % of diphenyl sulfide (DPS) was added to increase the refractive index of the core. Five types of fibers were fabricated; their characteristics are listed in Table I. The dyes were dispersed in the monomer before polymerization, and the 0.001 wt. % concentrations were at the saturation point without aggregation or precipitation. Fiber 1 is the target structure for which we expected emission from the cladding that was pumped by core emission. Fibers 2 and 3 were fabricated as controls to examine effects due to the presence of each dye. Fiber 2 lacks both donor and acceptor dyes, while fiber 3 lacks the acceptor dye in the cladding. Fiber 4 also has the target structure, but it has a lower numerical aperture (NA) compared to fiber 1 by doping with less DPS. Fiber 5 has a lower content of acceptor dye than fiber 1.

TABLE I. Test fibers and their compositions.

Fiber name	Rhodamine 6G (cladding)	Coumarin 540A (core)	Diphenyl sulfide (core) (wt. %)
Fiber 1	0.001 wt. %	0.001 wt. %	11
Fiber 2	…	…	11
Fiber 3	…	0.001 wt. %	11
Fiber 4	0.001 wt. %	0.001 wt. %	5
Fiber 5	0.0001 wt. %	0.001 wt. %	5

As done previously,[6,20,21] the polymerized preform was heat-drawn to a core/fiber diameter of 666/1000 μm and 1-m fibers were used for measurements. Figure 3 shows a schematic of the apparatus used to obtain the intensity balance between the core and cladding during stress application to a test fiber. Pigtail lasers with an approximate mode field of 3.2–4.3 μm (Precise Gauges LDS1003 series and LDS1004) were used as 406-nm, 532-nm, and 635-nm excitation sources. The 406-nm laser was optimum for efficiently exciting Coumarin 540A in the core (λ_{ex_D}). The 532-nm laser optimally excited Rhodamine 6G but weakly excited Coumarin 540A (λ_{ex_A}). The 635-nm laser excites neither dye. Each pigtail end was coupled to the test fiber with a direct contact to the core center of the test fiber to prevent cladding excitation. The fibers were subjected to various stresses by bending them in different loop diameters (1.5 cm, 3.0 cm, and 6.0 cm) created in the middle of the fiber length. The relaxed condition was straight with no loops. The output beam from the test fiber was analyzed using a near-field pattern (NFP) measuring system (Hamamatsu C9664-01G02) and a spectrophotometer (JASCO MV-3500).

Figure 4 shows NFPs of fibers 1–3 under non-stressed conditions for various excitation wavelengths. From Fig. 4(b), it is found that the NFPs of fiber 2 (containing no dyes) had significant intensity fluctuations corresponding to speckle patterns. The patterns were similar for all excitation wavelengths. In contrast, the NFP of fiber 3 had a homogeneous pattern only for 406-nm excitation [Fig. 4(c)]. Fiber 3 had only the core dye, which is excited by the 406 nm light (λ_{ex_D}).The other data in Fig. 4(c) show coarse speckle patterns similar to Fig. 4(b) for 532-nm and 635-nm excitations. This was because the dye was present in the core and the input wavelength matches its excitation wavelength. Thus, the absorption and emission activities will disturb the modal condition and its directivity.

Fiber 1 had Coumarin 540A doped in the core and Rhodamine 6G in the cladding and exhibited homogenous NFPs not only at 406 nm but also at 532-nm excitation as well [Fig. 4(a)]. Because 532 nm light excites Rhodamine 6G, some portion of the cladding material must have been present in the core. Hence, in the process of interfacial gel polymerization, a small amount of tubular inner surface of the cladding dissolved in the core monomer when the core monomer was in contact.

Figure 5 shows the change in the NFPs under various bending conditions. In each case, 406-nm light was used to excite Coumarin 540A in the core and the intensity was normalized with respect to the maximum intensity of the core. In Fig. 5(a), the patterns of fiber 1 exhibited increased

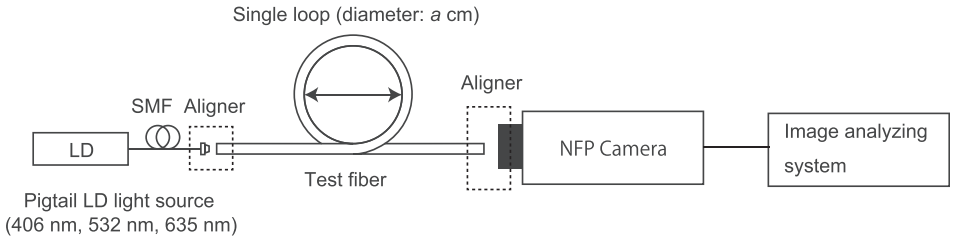

FIG. 3. Schematic of NFP apparatus for dye-doped POF at different bending stresses. The 1-m fiber was either straight (no stress) or bent in a single loop at the center. The loop diameter (a) was 1.5 cm, 3.0 cm, or 6.0 cm. A pigtail laser with a sufficiently small mode field was used to prevent cladding launches.

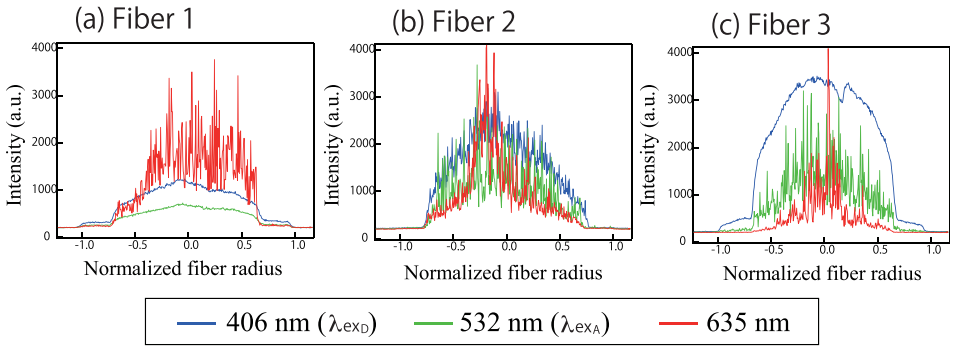

FIG. 4. NFPs of straight (no stress) (a) fiber 1, (b) fiber 2, and (c) fiber 3 for the input wavelengths of 406 nm (λ_{ex_D}), 532 nm (λ_{ex_A}), and 635 nm (excites neither dyes).

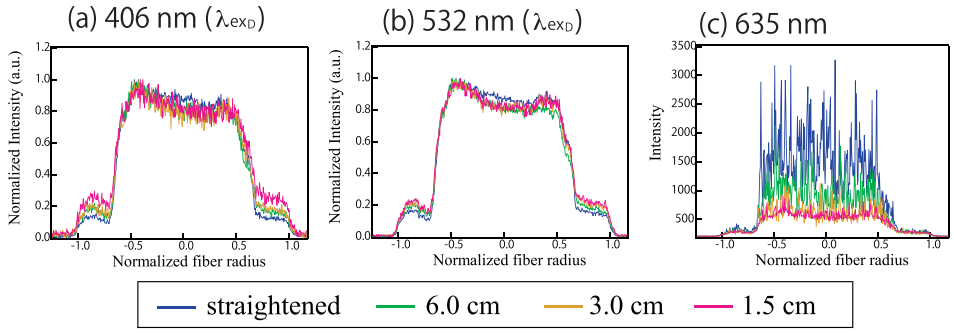

FIG. 5. Change in NFP of (a) fiber 1, (b) fiber 3, and (c) fiber 4 for different bending diameters. The excitation wavelength was 406 nm (λ_{ex_D}).

cladding intensity as the bending diameter was reduced. In contrast, there was almost no change in the patterns of fiber 3, as seen in Fig. 5(b). This suggests that the presence of the acceptor dye in the cladding realized the principle shown in Fig. 1. In Fig. 5(c), the fiber with both dyes and a lower NA exhibited even more cladding intensity as the bending diameter was reduced. This suggests that luminescence in the core was less confined with a lower NA and thus supplied more excitation light to the cladding.

Figure 6 shows NFPs of fiber 4 (lower NA) for various macro-bending conditions at different input wavelengths. The normalized intensity in Figs. 6(a) and 6(b) allows changes in cladding intensity to be compared clearly among these patterns. Figure 6(a) is identical to Fig. 5(c). Both cases show increased cladding intensity with stress as bending increased. The change was more significant in (a) than in (b), suggesting that these NFPs followed the principle of Fig. 1. However, according to that principle, the minor increase in cladding intensity seen in Fig. 6(b) was not expected. It may instead be attributed to unintentional contamination of Rhodamine 6G in the core suggested earlier in Fig. 4(a). Although it is a small amount, Rhodamine 6G in the core was excited when 532-nm light was present and was leaked to the cladding as the stress (bend) increased. Figure 6(c) shows the un-normalized pattern obtained when 635-nm light was used. The coarse speckle pattern suggests that 635 nm light did not interact with the dyes. The gradual decrease in the core intensity with increasing bending indicates that the optical power confined in the core was transferred to the cladding. However, because there was no

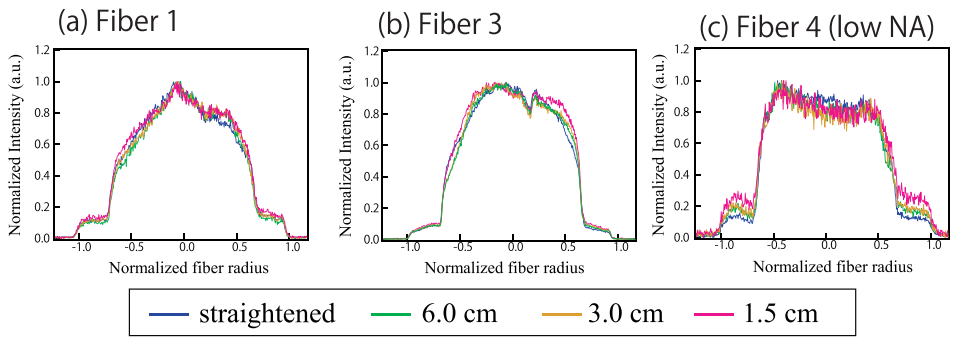

FIG. 6. Change in NFP of fiber 4 for different bending diameters at various input wavelengths.

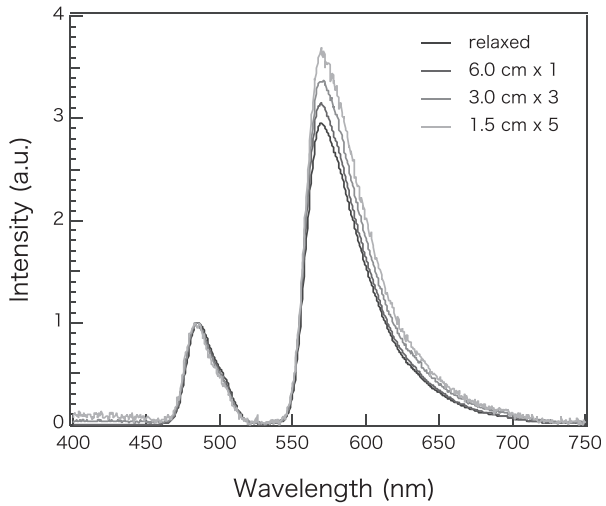

FIG. 7. Output spectra of fiber 5 for different bending conditions. The fiber was either relaxed (straightened) or bent in loops with specific diameters. The intensity was normalized with respect to the λ_{em_D} peak.

Rhodamine 6G excitation, a pronounced change in cladding intensity was not observed.

Figure 7 shows output spectra of fiber 5 for different bending conditions and for a 406-nm input. The intensity was normalized with respect to the λ_{em_D} peak to reveal changes in the Rhodamine 6G peak. The increase in the λ_{em_A} peak was confirmed as the bending increased, which agrees with the principle depicted in Fig. 1.

In conclusion, a stress sensor based on a dye-doped POF was fabricated, and its ability to sense stress via simple comparison of D/A emission intensities was demonstrated. A D/A pair of luminescent organic dyes (Coumarin 540A and Rhodamine 6G) were doped in the core and cladding of the fiber, respectively. Stress applied to the fiber by the way of bending could be detected as an increase in cladding intensity. Due to this deformation, emission from the core dye leaks to the cladding and excites the cladding dye. Changes in the NFP upon fiber bending were evaluated using different input wavelengths, some of which excite the dyes. The cladding intensity increased slightly when the core center was launched by λ_{ex_D}. Spectral analysis had shown a continuous increase in the donor peak as the bending increased. Observations confirmed that the fabricated structure can realize the proposed sensing principle. A low-NA fiber exhibited enhanced sensitivity, suggesting that the resolution of the sensor can be optimized by adjusting the waveguide parameters. The materials used here are not optimum for practical use. For example, the excitation and emission wavelengths of the dyes do not necessarily match the optical window of the host polymer. Thus, better choices of materials may be possible in future versions of the proposed fiber structure.

This work was supported by the MLIT Program for Promoting Technological Development of Transportation and Accurate maintenance for secure transportation infrastructures against aging and natural hazards, Development of robust transportation system against natural hazards, and "Development of organic-waveguide strain-sensor for health monitoring of shield tunneling process (Project No.: 2015-2)."

[1]B. Glisic and D. Inaudi, *Fiber Optic Methods* (Wiley, 2007), p. 19.
[2]G. P. Cimellaro, D. Solari, and M. Bruneau, Earthquake Eng. Struct. Dyn. **43**, 1763 (2014).
[3]I. Matsuda, J. Geogr. **122**, 1070 (2013).
[4]R. Furukawa, PCT Application. No. PCT/JP2016/059673, 2016.
[5]R. Furukawa, D. Mizorogi, K. Tsukada, E. Nihei, M. Matsuura, A. Inoue, A. Tagaya, and Y. Koike, "Stress-induced light leakage of rhodamine 6G doped polymer optical fiber," in 23rd International Conference on Plastic Optical Fibers (POF 2014), Kanagawa, Japan, 2014.
[6]R. Furukawa, A. Tagaya, S. Iwata, and Y. Koike, J. Phys. Chem. C **112**, 7946 (2008).
[7]U. Paek and R. Runk, J. Appl. Phys. **49**, 4417 (1978).
[8]R. Furukawa, A. Tagaya, S. Iwata, and Y. Koike, Jpn. J. Appl. Phys., Part 1 **93**, 103303 (2008).
[9]R. F. Kubin and A. N. Fletcher, J. Lumin. **27**, 455 (1982).
[10]K. Kuriki, T. Kobayashi, N. Imai, N. T. Tamura, Y. Koike, and Y. Okamoto, Polym. Adv. Technol. **11**, 612 (2000).
[11]I. Ayesta, M. A. Illarramendi, J. Arrue, I. Parola, F. Jiménez, J. Zubia, A. Tagaya, and Y. Koike, Polymers **9**, 90 (2017).
[12]E. J. Schimitschek, J. A. Trias, P. R. Hammond, and R. L. Atkins, Opt. Commun. **11**, 352 (1974).
[13]K. H. Drexhage and G. A. Reynolds, in Quantum Electronics Conference (1974), Paper No. F.1.
[14]J. A. Halsted and R. R. Reeves, Opt. Commun. **27**, 273 (1978).
[15]G. Jones, W. R. Jackson, and A. M. Halpern, Chem. Phys. Lett. **72**, 391 (1980).
[16]F. Bos, Appl. Opt. **20**, 1886–1890 (1981).
[17]H. Telle, W. Huffer, and D. Basting, Opt. Commun. **38**, 402–406 (1981).
[18]T. C. Eschrich and T. J. Morgan, Appl. Opt. **24**, 937–938 (1985).
[19]M. Sato, T. Ishigure, and Y. Koike, J. Lightwave Technol. **18**, 952 (2000).
[20]R. A. Furukawa, A. Tagaya, and Y. Koike, Appl. Phys. Lett. **112**, 7946 (2008).
[21]R. A. Furukawa, A. Tagaya, and Y. Koike, ACS Appl. Mater. Interfaces **7**, 388 (1982).